Original

Bergstroem, L.M.; Skoglund, S.; Danerloef, K.; Haramus, V.M.; Pedersen, J.S.:
The growth of micelles, and the transition to bilayers, in mixtures of a single-chain and a double-chain cationic surfactant investigated with small-angle neutron scattering
In: Soft Matter (2011) RSC Publishing

DOI: 10.1039/c1sm05760j

Soft Matter

Cite this: *Soft Matter*, 2011, **7**, 10935

www.rsc.org/softmatter

PAPER

The growth of micelles, and the transition to bilayers, in mixtures of a single-chain and a double-chain cationic surfactant investigated with small-angle neutron scattering

L. Magnus Bergström,*[a] Sara Skoglund,[a] Katrin Danerlöv,[b] Vasil M. Garamus[c] and Jan Skov Pedersen[d]

Received 26th April 2011, Accepted 7th September 2011
DOI: 10.1039/c1sm05760j

Self-assembly in aqueous mixtures of a single-chain (DTAB) and a double-chain cationic surfactant (DDAB) has been investigated with small-angle neutron scattering (SANS). Small oblate spheroidal micelles formed by DTAB grow with respect to width and length to form mixed ellipsoidal tablet-shaped micelles as an increasing fraction of DDAB is admixed into the micelles. The growth behaviour of the micelles is rationalized from the general micelle model in terms of three bending elasticity constants spontaneous curvature (H_0), bending rigidity (k_c) and saddle-splay constant ($\bar{k}_c$). It is found that micelles grow with respect to width, mainly as a result of decreasing k_cH_0, and in the length direction as a result of decreasing k_c. The micelles are still rather small, *i.e.* about 140 Å in length, as an abrupt transition to large bilayer aggregates is observed. The micelle-to-bilayer transition is induced by changes in aggregate composition and is observed to occur at a mole fraction of DDAB equal to about $x = 0.48$ in D_2O, which is a significantly higher value than previously observed for the same system in H_2O ($x = 0.41$). An abrupt micelle-to-bilayer transition is in agreement with predictions from the general micelle model, according to which an abrupt transition from micelles to bilayers is expected to occur at $\xi H_0 = 1/4$, where ξ is the thickness of the self-assembled interface, and we may conclude that $H_0(D_2O) > H_0(H_2O)$ for the system DDAB/DTAB in absence of added salt. Samples with bilayers are found to be composed of bilayer disks coexisting with vesicles. Disks are found to always predominate over vesicles with mass fractions about 70–90% disks and 10–30% vesicles. Micelles, disks and vesicles are observed to coexist in a few samples close to the micelle-to-bilayer transition.

1. Introduction

Surfactants are amphiphilic molecules composed of a hydrophilic and a lipophilic part that self-assemble above the so-called critical micelle concentration in an aqueous solvent to form self-assembled interfacial aggregates of different geometries. Two fundamentally different types of self-assembled interfacial aggregates, micelles and bilayers, have been observed to form in dilute aqueous solutions, depending on the chemical structure of the surfactants. Micelles are usually formed by surfactants with a comparatively large hydrophobic-lipophilic balance (HLB), for instance ionic or nonionic surfactants with a single aliphatic hydrocarbon chain, whereas various bilayer structures are formed by surfactants with a much smaller HLB, for instance a double-chain ionic surfactant.

In the present work, we investigate dilute mixtures of the single-chain cationic surfactant dodecyl trimethylammonium-bromide (DTAB) and the double-chain cationic surfactant didodecyl dimethylammouniumbromide (DDAB) using small-angle neutron scattering (SANS). It is known that DTAB form small oblate micelles in dilute aqueous solutions in the absence of added salt,[1] whereas large bilayer fragments and vesicles have been observed in dilute solutions of pure DDAB dissolved in water.[2] In this particular work, we carry out a comprehensive investigation where we follow the growth behaviour of micelles, and the subsequent transformation from micelles to bilayers, as an increasing amount of DDAB is added to DTAB solutions, or as a sample with micelles is simply diluted.

The system we have chosen to study, *i.e.* the dilute regime in mixtures of DTAB and DDAB, has recently been investigated in detail by Aratano *et al.*[3] using surface tension, electrical conductivity, turbidity and cryotransmisson electron microscopy (CRYO-TEM). They observed a transition from monomers to vesicles (as identified from CRYO-TEM images) to micelles as the total surfactant concentration was raised at a fixed surfactant

[a]*Surface and Corrosion Science, Chemical Science and Engineering, Royal Institute of Technology, SE-100 44 Stockholm, Sweden. E-mail: magnusbe@kth.se; Fax: +46 8 20 82 84; Tel: +46 8 790 99 21*
[b]*YKI, Institute for Surface Chemistry, SE-114 86 Stockholm, Sweden*
[c]*Helmholtz-Zentrum Geesthacht: Centre for Materials and Coastal Research, D-215 02 Geesthacht, Germany*
[d]*Department of Chemistry and iNANO Interdisciplinary Nanoscience Center, Aarhus University, DK-8000 Aarhus, Denmark*

molar ratio in the solution. At higher fractions of DDAB a regime consisting of small aggregates was observed between the monomer and the vesicle regimes. Vesicles were seen to coexist with micelles or small aggregates in rather narrow intermediate regimes. More recently, the abrupt transition from rather small micelles to large bilayer aggregates in this system was investigated with static light scattering.[4] From calculations using the Poisson–Boltzmann mean field theory it was possible to demonstrate that the micelle-to-bilayer transition is induced by changes in surfactant composition in the self-assembled interfacial aggregates and always occur at an aggregate mole faction of DDAB equal to $x = 0.41$.[4]

A significant part of the present work is a detailed study of the growth behaviour of mixed surfactant micelles as a function of surfactant composition. In some recent theoretical works we have developed a novel theory for the self-assembly of surfactant molecules by means of combining thermodynamics of self-assembly and bending elasticity theory.[5–11] According to this approach, it follows that the structural behaviour (size, geometry, flexibility, polydispersity *etc.*) of self-assembled interfacial aggregates may be deduced from the three bending elasticity constants spontaneous curvature (H_0), bending rigidity (k_c) and saddle-splay constant ($\bar{k}_c$), respectively. For instance, it is demonstrated that micelles are expected to predominate as the spontaneous curvature exceeds a certain value equal to $H_0 = 1/4\xi$, where ξ is the thickness of the self-assembled interface, whereas bilayers are predicted to be the predominant structure as H_0 falls below $1/4\xi$.[5,8,10]

2. Materials and methods

2.1 Materials

Dodecyl trimethylammoniumbromide (>99%, GC) was obtained from Sigma whereas didodecyl dimethylammouniumbromide (>98%, GC) was obtained from Fluka. Both surfactants were used without further purification. Heavy water (D_2O) with 99.9 atom % D was purchased from Aldrich Chemical Company.

2.2 Sample preparation

Stock solutions containing dodecyl trimethylammoniumbromide (DTAB) and didodecyl dimethylammouniumbromide (DDAB) with different surfactant compositions ranging from $y \equiv$ [DDAB]/([DTAB] + [DDAB]) = 0 to $y = 0.40$ were prepared by simply mixing the surfactants with water to yield an overall surfactant concentration [DTAB] + [DDAB] = 30 mM. The final samples were obtained by means of diluting the stock solutions with water to obtain any desired total surfactant concentration c_t. Each sample was equilibrated at least 48 h at room temperature (23 °C). Heavy water (D_2O) was chosen as solvent in order to minimize the incoherent background from hydrogen and obtain a high scattering contrast.

2.3 Methods

Small-angle neutron scattering (SANS) experiments were carried out at the SANS-1 instrument at the Geesthach Neutron Facility GeNF, Geesthacht, Germany. A range of magnitudes of the scattering vector q from 0.005 to 0.25 Å^{-1} was covered by three or four combinations of sample-to-detector distances (0.7–9.7 m) at a neutron wavelength of 8.5 Å. The wavelength resolution was $\Delta\lambda/\lambda = 10\%$ (full-width-at-half-maximum value).

The samples were kept in quartz cells (Hellma) with a path length of either 2 or 5 mm. The raw spectra were corrected for background from the solvent, sample cell and other sources by conventional procedures.[12] The two-dimensional isotropic scattering spectra were azimuthally averaged, converted to an absolute scale and corrected for detector efficiency by dividing by the incoherent scattering spectra of pure water measured in a 1 mm cell.[13] The scattering intensity was normalized by dividing with the concentrations in g mL^{-1} of solute (DTAB and DDAB).

Throughout the data analyses corrections were made for instrumental smearing.[14,15] For each instrumental setting the ideal model scattering curves were smeared by the appropriate resolution function when the model scattering intensity was compared with the measured one by means of least-squares methods. The parameters in the model were optimized by means of conventional least-squares analysis an their errors were calculated with conventional methods.[16,17] The quality of the fits were measured in terms of the reduced chi-squared parameter defined as

$$\chi^2 = \frac{1}{N-M}\sum_{i=1}^{N}\left(\frac{I_{exp}(q_i) - I_{mod}(q_i)}{\sigma_i}\right)^2 \quad (1)$$

where $I_{exp}(q_i)$ and $I_{mod}(q_i)$ are the experimental and model intensities, respectively, at a scattering vector modulus q_i, σ_i is the statistical uncertainties on the data points, N is the total number of data points and M is the number of parameters optimized in the model fit.

The average excess scattering length density per unit mass of solute for DDAB (Surfactant 1) in D_2O, $\Delta\rho_m = -7.01 \times 10^{10}$ cm g^{-1}, was calculated using the appropriate molecular volume $\hat{v}_1 =$ 810 Å^3 and molecular weight $M_w = 462.65$ g mol^{-1} of the surfactant monomer.[18] The corresponding quantities for DTAB (Surfactant 2) are $\Delta\rho_m = -6.37 \times 10^{10}$ cm g^{-1}, $\hat{v}_2 = 491$ Å^3 and $M_w = 308.35$ g/mol.

Static Light Scattering (SLS) measurements were carried out with a BI-200SM goniometer from Brookhaven Instruments attached to a water-cooled Lexel 95-2 laser with maximum power of 2 W and wavelength 514.5 nm. Experiments were carried out at 29 different angles in the range of $15° \leq \theta \leq 155°$, corresponding to q values in the range of 4.26×10^{-4} Å$^{-1} \leq q \leq 31.8 \times 10^{-4}$ Å^{-1}. For each angle the sample was measured a maximum of fifteen individual times out of which the five with the lowest intensities were picked out and subsequently averaged. The SLS data were then converted to absolute neutron units using toluene as a reference standard before combined and analysed together with SANS data.

3. Data analyses

The scattering cross section per unit mass of solute as a function of scattering vector q for a sample of monodisperse non-spherical particles can be written as follows

$$\frac{d\sigma_m(q)}{d\Omega} = \Delta\rho_m^2 M_w P(q)[1 + \beta(q)(S(q) - 1)] \quad (2)$$

where $\Delta\rho_m$ is the difference in scattering length per unit mass solute between particles and solvent, M_w is the molar mass of a particle and $P(q) \equiv \langle F^2(q)\rangle_0$ is the orientational averaged form

factor.[17] The structure factor $S(q)$ is included using a so-called decoupling approximation, where $\beta(q) \equiv \langle F(q)\rangle_0^2/\langle F^2(q)\rangle_0$, valid for particles with small anisotropy.[19]

Rather small micelles are formed in samples with high fractions of DTAB in the aggregates, and the corresponding SANS data were best fitted using a model for triaxial ellipsoids with half axis a, b and c. The orientational averaged form factor for triaxial ellipsoids equals

$$\langle F^2(q)\rangle_0 = \frac{2}{\pi}\int_0^{\pi/2}\int_0^{\pi/2} F^2(q, r(a,b,c,\phi,\theta))\sin\phi d\phi d\theta \quad (3)$$

where $F(q, r) = 3[\sin(qr) - qr\cos(qr)]/(qr)^3$ and $r(a,b,c,\phi,\theta) = \sqrt{(a^2\sin^2\theta + b^2\cos^2\theta)\sin^2\phi + c^2\cos^2\phi}$.[20]

Interactions were taken into account by means of using a structure factor $S(q)$ including repulsive excluded volume interactions as well as electrostatic double-layer forces as derived by Hayter and Penfold[21] from the Ornstein–Zernike equation in the rescaled mean spherical approximation.[22]

An abrupt transition from micelles to bilayers is found as the fraction of DDAB is increased beyond a certain value, and the corresponding scattering data were best fitted with a model of coexisting bilayer disks and vesicles (= spherical bilayer shells). For large aggregates, the corresponding scattering cross-section may be written as

$$\frac{d\sigma(q)}{d\Omega} = \Delta\rho_m^2\left[f_d M_d P_b\langle V_d^2 P_d\rangle + (1-f_d)M_v P_b\langle V_v^2 P_v\rangle\right] \quad (4)$$

where f_d and $f_v = 1 - f_d$ are the relative mass fractions of bilayer disks and vesicles, respectively.[23]

The form factor of a bilayer cross-section is given by

$$P_b(q\xi) = \left(\frac{\sin q\xi}{q\xi}\right)^2 \quad (5)$$

where we have assumed disks and vesicles to have identical half bilayer thickness ξ.

$$\langle V_d^2 P_d\rangle = \int N_d(R)V_d^2(R)P_d(qR)dR \quad (6)$$

with

$$P_d(qR) = \frac{2[1 - B_1(2qR)/qR]}{(qR)^2} \quad (7)$$

is the form factor for a collection of polydisperse infinitely thin circular disks with a number-weighted Gaussian size distribution, *i.e.*

$$N_d(R) = \frac{1}{\sigma_d\sqrt{2\pi}}e^{-(R-R_d)^2/2\sigma^2} \quad (8)$$

where σ_d is the standard deviation with respect to disk radius R and R_d is the average disk radius.[17,24] $B_1(x)$ is the Bessel function of first order.

$$\langle V_v^2 P_v\rangle = \int N_v(R)V_v^2(R)P_v(qR)dR \quad (9)$$

with

$$P_v(qR) = \left(\frac{\sin qR}{qR}\right)^2 \quad (10)$$

is the form factor of polydisperse and infinitely thin vesicles with radius R, where we have assumed the vesicle size distribution to follow a Schultz distribution, *i.e.*[17,25]

$$N_v(R) = \frac{2R^{2z+1}}{z!}\left(\frac{z+1}{R_v^2}\right)^{z+1}e^{-R^2(z+1)/R_v^2} \quad (11)$$

where R_v is the average vesicle radius.

The scattering data for a few samples in proximity to the micelle-to-bilayer transition could only be fitted with a model for coexistence between micelles, disks and vesicles, *i.e.*

$$\frac{d\sigma(q)}{d\Omega} = \Delta\rho_m^2\left[f_d M_d P_b\langle V_d^2 P_d\rangle + f_v M_v P_b\langle V_v^2 P_v\rangle + (1-f_d-f_v)M_m P_m\right] \quad (12)$$

where $f_m = 1 - f_d - f_v$ is the mass fraction of micelles. The micelles in eqn (12) are modelled as long rods and the corresponding form factor can be written as a product

$$P_m(q) = P_{cs}(q)P_r(q) \quad (13)$$

where

$$P_{cs}(q,a,b) = \frac{2}{\pi}\int_0^{\pi/2}\left(\frac{2B_1(qr(a,b,\phi))}{qr(a,b,\phi)}\right)^2 d\phi \quad (14)$$

with

$$r(a,b,\phi) = \sqrt{a^2\sin^2\phi + b^2\cos^2\phi} \quad (15)$$

accounts for an elliptical cross-section with half axes a and b.[1,26] The form factor of an infinitely thin rod with length L is given by[27]

$$P_r(qL) = 2\mathrm{Si}(qL) - 4\sin^2(qL/2)/(qL)^2 \quad (16)$$

where

$$\mathrm{Si}(x) = \int_0^x \frac{\sin t}{t}dt \quad (17)$$

M_d, M_v and M_m in eqn (4) and (12) denote the apparent molar masses of bilayer disks, vesicles and micelles, respectively. Interparticle interactions are difficult to include in such complicated samples and have been neglected in the analysis. The average scattering length density contrast $\Delta\rho_m$ depends, in principle, on the surfactant composition in the aggregates. It is not possible to determine both $\Delta\rho_m$ and the surfactant composition in a single geometrical part. However, since the two surfactants have very similar scattering length densities, f_v, f_d and f_m are expected to be accurately determined by simply setting $\Delta\rho_m$ to the same value for the different aggregate types. Likewise, the density is expected to be independent of aggregate composition and, as a result, we may relate the various molar masses as $M_d/M_v = V_d/V_v$ and $M_d/M_m = V_d/V_m$, where the volumes of bilayer disks, vesicles and micelles are given by the following geometrical relations $V_d = 2\xi\pi R_d^2$, $V_v = 8\pi R_v^2\xi$ and $V_m = \pi abL$, respectively.

The number of fit parameters, including the absolute scale scattering intensity at $q = 0$ and residual incoherent background scattering, is $M = 6$–9. The number of data points is about $N = 60$–100. For a few samples where SLS data are included $M = 8$–11 (the additional fitting parameters are R_d and σ_d/R_d) and

$N \approx 130$. We have aimed at keeping our models as simple as possible and always been careful not to introduce any additional fitting parameters unless they give rise to a significantly improved quality of the model fit.

Both micelles and bilayer aggregates were fitted with a homogeneous one-shell model and the quality of the fits could not be improved using a core-and-shell model or a model taking into account internal differences in scattering length densities in the micelle core. This is not surprising considering that the head groups of both DTAB and DDAB have almost identical scattering length densities as the surfactant tails and that the head groups only protrude a few angstroms outside the core. Likewise, the difference in scattering length densities between methylene ($–CH_2–$) and methyl ($–CH_3$) groups is small as compared with the difference between hydrocarbon and deuterium oxide. Moreover, the hydrocarbon core is liquid-like which means that methylene and methyl groups must to a large extent be randomly mixed inside the hydrocarbon core and corresponding effects tend to become out-averaged. The small difference in scattering length densities between the two surfactants (DTAB and DDAB) also imply that effects due to partial segregation of surfactants in geometrically inhomogeneous self-assembled interfacial aggregates[7] (the fraction of DTAB is expected to be higher in more curved regimes of the aggregates) becomes is negligible.

4. Results and discussion

SANS data together with model fits are shown in Fig. 1–3. The growth of rather small micelles, followed by an abrupt transition to bilayers, is clearly seen as the fraction of DDAB in solution is increased at a fixed total surfactant concentration (*cf.* Fig. 1 and 2) or the total surfactant concentration is decreased at a fixed solution composition (*cf.* Fig. 3). The results of our least-square model fitting analyses are summarized in Table 1.

SANS data for samples with micelles were best fitted with a model for general (triaxial or scalene) ellipsoids with half axes a, b and c. Typical errors in the fitting procedure are less than ± 0.5 Å for a and b, and ± 1 Å for c. This model has previously been successfully employed for similar, pure and mixed, surfactant systems.[1,23,26,28] By means of comparing the agreement between scattering data and different geometrical shapes of surfactant micelles (sphere, oblate and prolate spheroids, triaxial ellipsoids, one and two-shell models), we were able to conclude that the triaxial ellipsoidal shape gives a significantly better agreement between model and data than the other geometries. For identical reasons we are able to conclude that micelles formed in mixtures of DTAB and DDAB are tablet-shaped, *i.e.* with a distinct thickness, width and length, respectively, that become shaped as oblate spheroids in the limiting case of pure DTAB micelles. As a matter of fact, oblate and prolate spheroid shapes are inherent as special cases in the triaxial ellipsoid model. The comparatively small errors on the half axes fitting parameters demonstrate that the ellipsoidal shape is significantly more consistent with our scattering data than prolate or oblate spheroid shape. Models for monodisperse or polydisperse spheres give an even worse agreement between model and data.[1] Spherical micelles can also be ruled out from simple geometrical reasons and the fact that the radius of a sphere may not exceed the length of a fully stretched surfactant molecule.[29]

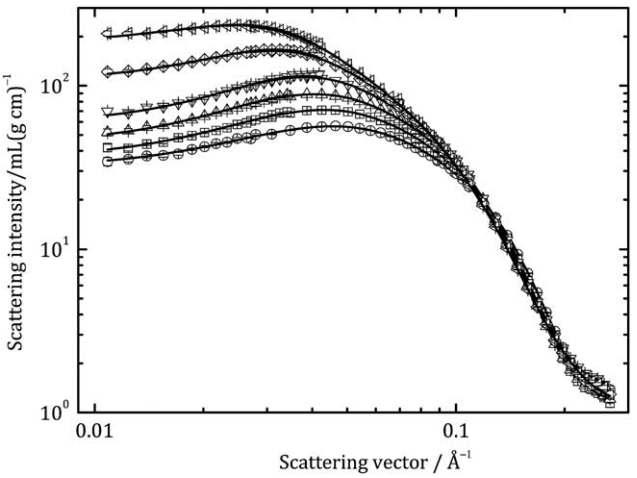

Fig. 1 Normalized scattering cross section as a function of the scattering vector q for mixtures of DTAB and DDAB in D_2O for a given total surfactant concentration c_t = [DDAB] + [DTAB] = 30 mM. The composition of the samples are y = [DDAB]/([DDAB] + [DTAB]) = 0 (pure DTAB, circles), $y = 0.05$ (squares), $y = 0.10$ (up triangles), $y = 0.15$ (down triangles), $y = 0.20$ (diamonds) and $y = 0.25$ (left triangles). Individual symbols represent SANS data obtained for different sample-detector distances. The solid lines represent the best available fit with a model for an oblate spheroid (circles) or general ellipsoid (squares, triangles and diamonds). The results of the fits are given in Table 1. The quality of the fits as measured by χ^2 are 5.0 (circles), 5.1 (squares), 4.1 (up triangles), 8.0 (down triangles), 12.7 (diamonds) and 9.5 (left triangles).

Pure DTAB in (heavy) water and absence of added salt is found to form oblate micelles with $a = 14$ Å and $b = 24$ Å at 23 °C. The micelles are slightly larger, but with the same oblate

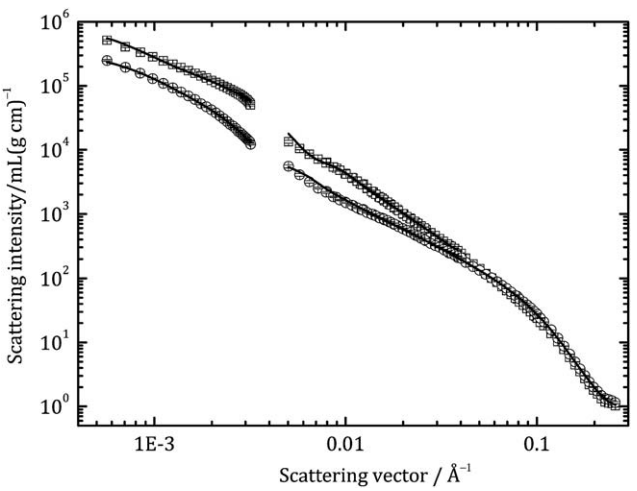

Fig. 2 Normalized scattering cross section as a function of the scattering vector q for mixtures of DTAB and DDAB in D_2O for a given total surfactant concentration c_t = [DDAB] + [DTAB] = 30 mM. The composition of the samples are $y = 0.30$ (circles) and $y = 0.40$ (squares). Individual symbols represent SANS data obtained for different sample-detector distances and SLS data. The solid lines represent the best available fit with a model for coexisting bilayer disks and bilayer vesicles (squares) and coexisting disks, vesicles and rodlike micelles (circles). The results of the fits are given in Table 1. The quality of the fits as measured by χ^2 are 7.7 (circles) and 3.5 (squares).

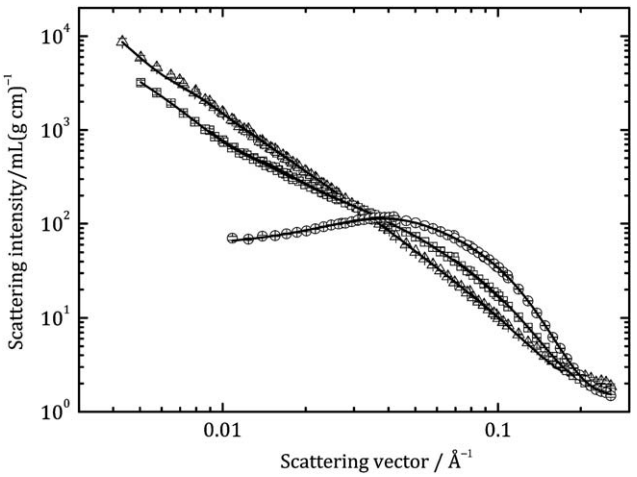

Fig. 3 Normalized scattering cross section as a function of the scattering vector q for mixtures of DTAB and DDAB in D_2O for a given mole fraction of DDAB in solution y = [DDAB]/([DDAB] + [DTAB]) = 0.15. The overall surfactant concentration of the samples are c_t = [DDAB] + [DTAB] = 30 mM (circles), c_t = 15 mM (squares) and c_t = 7.5 mM (up triangles). Individual symbols represent SANS data obtained for different sample-detector distances. The solid lines represent the best available fit with a model for a general ellipsoid (circles), coexisting bilayers disks, bilayer vesicles and rodlike micelles (squares) and coexisting disks and vesicles (triangles). The results of the fits are given in Table 1. The quality of the fits as measured by χ^2 are 8.0 (circles), 4.3 (squares) and 1.8 (triangles).

spheroid geometry, as previously found for DTAB micelles at 40 °C.[1] As an increasing amount of DDAB is added, the micelles become increasingly more elongated. The half axis related to the length of the micelles (c) increases significantly with increasing DDAB mole fraction whereas the half axis related to the width (b) increases only slightly as y is increased [*cf.* Fig. 4]. The thickness of the micelles (equivalent to a) increases slightly as a small amount of DDAB is added, but is approximately constant with respect to composition at higher fractions of DDAB. The former effect is most likely a consequence of the reduction of unfavourable head group interactions tending to decrease the area per head group and, as a result, increase the thickness of the self-assembled interface. The presence of a single type of micelle (the general micelle), rather than different types of micelles coexisting with each other, is supported by previous surface tension studies by Aratono *et al.*[3] on the same system. In Table 1 we have also included the micelle aggregation number as calculated from the geometrical relation $N_{agg} = 4\pi abc/3[x\hat{v}_1 + (1-x)\hat{v}_2]$, where $\hat{v}_1$ and $\hat{v}_2$ are the molecular volumes of the two surfactants and x is the mole fraction of Surfactant 1 (DDAB) in the micelles.

Notably, the micelles never grow larger than ellipsoids with a half axis related to length equal to c = 70 Å. Rather than further growing into long wormlike or threadlike micelles, the comparatively small micelles abruptly transform into much larger bilayer aggregates. In a recent paper we have demonstrated that the free surfactant concentrations as well as composition in the self-assembled interfacial aggregates may be accurately calculated from the Poisson–Boltzmann theory.[4] In accordance, we have in Table 1 included the mole fraction of DDAB in the aggregates (denoted x) as calculated from the critical micelle concentration (cmc) values of DDAB (Surfactant 1) and DTAB (Surfactant 2) in H_2O (cmc_1 = 0.085 mM and cmc_2 = 15.4 mM, respectively).[4] It is clearly seen that the growth of micelles, followed by a transition to bilayers, is strongly correlated to the fraction of DDAB in the aggregates.

In addition to the three half axes, the model fits for samples with micelles were also optimized with respect to the concentration of surfactant incorporated in micelles (c_{mic}), electrolyte concentration (c_{el}) and effective charge (z_{eff}). These parameters are related to the structure factor which brings down the scattering intensities at low-q values. The geometrical cross-section dimensions, *i.e.* thickness and width, on the other hand, influence the scattering data in the high-q regime. As a result, taking into account inter-micelle interactions in our data analysis have virtually no influence on thickness and width as obtained from our model fits.[1] However, the structure factor may have a slight influence on the length of the micelles, the quantity of which is influenced by the scattering behaviour at lower q-values, in so far the micelles become substantially elongated. The low impact of structure factor effects on geometrical dimensions is demonstrated by the low errors of the half axes fitting parameters (less than 1 Å, see above), as obtained from our analyses. The negligible influence of inter-micelle interactions on the geometrical shape of micelles, as obtained from our SANS data analyses, is also supported by our previous investigations of tablet-shaped micelles in solutions with different electrolyte concentrations.[1]

In our present analyses we have fitted all three parameters c_{mic}, c_{el} and z_{eff}. This was done in order to obtain best possible agreement between data and model, and to minimize correlation effects between geometrical properties related to the form factor and structure factor effects due to interactions between micelles. The interpretation of these fitting parameters might, however, be obscured by the fact that the rescaled mean spherical approximation (RMS) model has been employed in the data analysis. This model accounts for repulsive double-layer force interactions among spherical micelles, although non-spherical micelles are present in our particular system. Nevertheless, we obtain rather realistic values for the corresponding fitting parameters. The effective charge is found to be about 10–30% of the ideally charged micelles ($\alpha \equiv z_{eff}/N_{agg}$ = 0.10–0.30), whereas c_{mic} (= 4–21 mM) and c_{el} = (5–15 mM) assume reasonable values considering the total surfactant concentration (7.5–30 mM) and cmc of pure DTAB (15.4 mM). The errors of these fitting parameters are about $\Delta\alpha = \pm 0.03$, $\Delta c_{mic} = \pm 1$ mM and $\Delta c_{el} = \pm 2$ mM, but may occasionally be larger as the inter-micelle interactions become weaker. The interactions in the sample [y = 0.10, c_t = 15 mM] appeared to be too small in magnitude to determine c_{el} and z_{eff}.

Lusvardi *et al.*[30] have previously investigated mixed micelles formed by DTAB and DDAB with SANS. They were investigating samples in the regime $0 < y < 0.3$ at rather high surfactant concentrations (c_t = 200 and 400 mM, respectively), *i.e.* in regimes where only micelles exist. In their data analyses they only considered biaxial spheroidal geometry. However, since they only measured scattering vectors up to $q = 0.22$ Å^{-1} it might be difficult to distinguish biaxial spheroidal from triaxial ellipsoidal shape. Nevertheless, a discrepancy between data and model fit, which is increasing in magnitude with increasing micelle size, is evident in the high-q range of their SANS data.

Table 1 Results from least-square model fitting analyses of SANS data. Dimensional properties (a, b, c, ξ, R_v and R_d) are given in Å units

	$y = 0$	$y = 0.05$	$y = 0.10$	$y = 0.15$	$y = 0.20$	$y = 0.25$	$y = 0.30$	$y = 0.35$	$y = 0.40$
30 mM	Micelles	Micelles	Micelles	Micelles	Micelles	Micelles	Micelles & Bilayers	Micelles & Bilayers	Bilayers
	$a = 14.1$ $b = 23.7$ $N_{agg} = 68$ $\alpha = 0.13$ $c_{mic} = 21$ mM $c_{el} = 7$ mM	$a = 14.7$ $b = 23.8$ $c = 27.4$ $N_{agg} = 77$ $\alpha = 0.10$ $c_{mic} = 20$ mM $c_{el} = 6$ mM $x = 0.10$	$a = 15.4$ $b = 23.5$ $c = 31.8$ $N_{agg} = 88$ $\alpha = 0.13$ $c_{mic} = 19$ mM $c_{el} = 6$ mM $x = 0.18$	$a = 15.6$ $b = 23.9$ $c = 37.6$ $N_{agg} = 102$ $\alpha = 0.17$ $c_{mic} = 18$ mM $c_{el} = 8$ mM $x = 0.26$	$a = 15.7$ $b = 25.3$ $c = 51.1$ $N_{agg} = 141$ $\alpha = 0.31$ $c_{mic} = 12$ mM $c_{el} = 15$ mM $x = 0.34$	$a = 15.4$ $b = 27.2$ $c = 71.2$ $N_{agg} = 201$ $\alpha = 0.19$ $c_{mic} = 10$ mM $c_{el} = 11$ mM $x = 0.41$	$f_m = 0.48$ $f_d = 0.45$ $f_v = 0.07$ $a = 13.3$ $b = 28.0$ $\xi = 12.7$ $R_d = 1540$ $\sigma_d/R_d = 0.63$ $R_v = 710$ $\sigma_v/R_v = 0.36$ $x = 0.48$	$f_m = 0.33$ $f_d = 0.54$ $f_v = 0.13$ $a = 13.2$ $b = 28.0$ $\xi = 12.8$ $R_d = 1210$ $\sigma_d/R_d = 0.48$ $R_v = 370$ $\sigma_v/R_v = 0.57$ $x = 0.54$	$f_d = 0.61$ $f_v = 0.39$ $\xi = 12.7$ $R_d = 1990$ $\sigma_d/R_d = 0.54$ $R_v = 440$ $\sigma_v/R_v = 0.48$ $x = 0.59$
15 mM	Micelles (20 mM) $a = 13.1$ $b = 23.7$ $N_{agg} = 63$ $\alpha = 0.12$ $c_{mic} = 11$ mM $c_{el} = 7$ mM	Micelles $a = 14.4$ $b = 24.8$ $c = 35.2$ $N_{agg} = 89$ $\alpha = 0.16$ $c_{mic} = 4$ mM $c_{el} = 5$ mM $x = 0.30$	Micelles $a = 15.8$ $b = 25.3$ $c = 54.0$ $N_{agg} = 144$ $c_{mic} = 2$ mM $x = 0.44$	Micelles & Bilayers $f_m = 0.55$ $f_d = 0.41$ $f_v = 0.04$ $a = 13.6$ $b = 25.5$ $\xi = 13.2$ $R_v = 270$ $\sigma_v/R_v = 0.40$ $x = 0.52$	Bilayers $f_d = 0.73$ $f_v = 0.27$ $\xi = 12.3$ $R_v = 280$ $\sigma_v/R_v = 0.48$ $x = 0.59$	Bilayers $f_d = 0.78$ $f_v = 0.22$ $\xi = 13.0$ $R_v = 240$ $\sigma_v/R_v = 0.52$ $x = 0.64$	Bilayers $f_d = 0.85$ $f_v = 0.15$ $\xi = 13.0$ $R_v = 430$ $\sigma_v/R_v = 0.48$ $x = 0.69$	Bilayers $f_d = 0.81$ $f_v = 0.19$ $\xi = 13.0$ $R_v = 440$ $\sigma_v/R_v = 0.41$ $x = 0.74$	Bilayers $f_{di} = 0.80$ $f_v = 0.20$ $\xi = 12.9$ $R_v = 480$ $\sigma_v/R_v = 0.37$ $x = 0.78$
7.5 mM	—	Bilayers $f_d = 1.0$ $\xi = 12.3$ $x = 0.79$	Bilayers $f_d = 0.90$ $f_v = 0.10$ $\xi = 12.6$ $R_v = 430$ $\sigma_v/R_v = 0.62$ $x = 0.82$	Bilayers $f_d = 0.87$ $f_v = 0.13$ $\xi = 12.8$ $R_v = 500$ $\sigma_v/R_v = 0.43$ $x = 0.84$	Bilayers $f_d = 0.93$ $f_v = 0.07$ $\xi = 13.0$ $R_v = 520$ $\sigma_v/R_v = 0.39$ $x = 0.86$	Bilayers $f_d = 0.90$ $f_v = 0.10$ $\xi = 12.9$ $R_v = 520$ $\sigma_v/R_v = 0.38$ $x = 0.88$	Bilayers $f_d = 0.85$ $f_v = 0.15$ $\xi = 13.0$ $R_v = 600$ $\sigma_v/R_v = 0.29$ $x = 0.90$	Bilayers $f_d = 0.74$ $f_v = 0.26$ $\xi = 13.1$ $R_v = 390$ $\sigma_v/R_v = 0.44$ $x = 0.91$	Bilayers $f_d = 0.70$ $f_v = 0.30$ $\xi = 12.8$ $R_v = 470$ $\sigma_v/R_v = 0.40$ $x = 0.92$

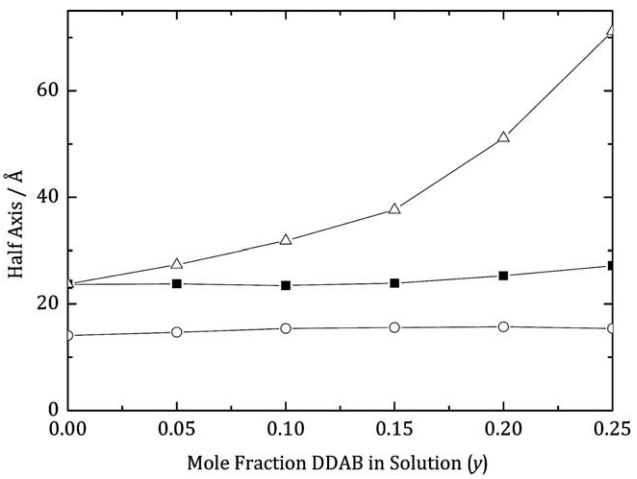

Fig. 4 Half axes related to the thickness a (circles), width b (squares) and length c (triangles), as obtained from the least square fitting analyses of SANS data, plotted against the mole fraction of DDAB in solution (y) for a given total surfactant concentration c_t = [DDAB] + [DTAB] = 30 mM.

Our observation of an abrupt transition from micelles to large bilayer vesicles or disks [*cf.* Fig. 1–3 and Table 1] resembles a similar transition in mixtures of an anionic and a cationic surfactant,[23,25] and our recent study of DDAB/DTAB mixtures in H_2O[4] supports the idea that the transformation from micelles to bilayers is induced by internal aggregate properties, *i.e.* a change in aggregate composition, rather than, for instance, inter-aggregate interactions. The aggregate composition is expected to influence bending elasticity properties and, as a matter of fact, an abrupt transition from micelles to various bilayer structures, including vesicles, have been predicted by means of combining the curvature elasticity approach of calculating the free energy of self-assembled interfacial aggregates with thermodynamics of self-assembly. In accordance, a micelle-to-bilayer transition is predicted to occur at a spontaneous curvature equal to $H_0 = 1/4\xi$, where ξ is the thickness of the self-assembled interface.[5,8,10]

Despite the fact that the cmc of DTAB has been found to be, within experimental errors, equal in H_2O and D_2O,[31] we can observe a slight difference in structural behaviour between surfactants dissolved in H_2O (SLS measurements in ref. 4), and D_2O (SANS measurements in the present work). In accordance, micelles were seen to form at [$y = 0.10$, $c_t = 15$ mM] and [$y = 0.25$, $c_t = 30$ mM] in D_2O, whereas bilayers were observed at the very same surfactant concentrations in H_2O. From our results shown in Table 1, it is seen that only micelles are present at $x = 0.44$ whereas bilayer aggregates have started to form at $x = 0.48$. These values are considerably higher than what we found in H_2O, *i.e.* bilayers starting to form at $x = 0.41$.[4] This means that the transition from micelles to bilayers must be significantly shifted towards higher fractions of DDAB in D_2O as compared to H_2O. Comparing with the fundamental equation for the micelle-to-bilayer transition, $\xi H_0 = 1/4$, we may conclude that the spontaneous curvature must be larger for DTAB/DDAB mixtures in D_2O as compared to the same surfactant mixture in H_2O, *i.e.* $H_0(D_2O) > H_0(H_2O)$.

Samples consisting of bilayers were best fitted with a model for coexisting bilayer disks and vesicles. From our results shown in Table 1, it is seen that the samples mainly consist of bilayer disks (70–90%) coexisting with a smaller fraction of vesicles (10–30%). The presence of a small amount of vesicles is indicated by a small bump, or inflexion point, in the SANS data at about, or slightly below, $q = 0.01$ Å^{-1} [*cf.* Fig. 2 and 3]. We have previously found bilayer disks and vesicles to coexist in mixtures of two oppositely charged surfactants (sodium dodecyl sulfate and DDAB), although approximately equal amounts of vesicles and disks were observed in this particular system.[23] The errors of f_d and f_v in our least-square model fit analyses are about ±0.05–0.10.

The half bilayer thickness was found to be about $\xi = 13$ Å, without any systematic tendencies with respect to surfactant composition or concentration, with an error less than about $\Delta\xi = \pm 0.5$ Å. The vesicle radius was found to be in the range 250–700 Å, whereas the polydispersity in terms of the (number-weighted) relative standard deviation $\sigma_v/R_v \approx 0.4$, with errors about $\Delta R_v = \pm 10$ Å and $\Delta(\sigma_v/R_v) = \pm 0.10$–0.15, respectively. For the samples $y = 0.30$, 0.35 and 0.40 at $c_t = 30$ mM, we have also included static light scattering (SLS) data in our model fitting analyses, which has enabled us to determine the apparent bilayer disk radius, roughly corresponding to about 1200–2000 Å [*cf.* Fig. 2]. However, since we have not, in our analysis, taken into account inter-aggregate interactions, the real size of the bilayer disks is expected to be significantly larger. The disk polydispersity σ_d/R_d is also influenced by the scattering behaviour of the SLS data in the low-q regime. SLS data for the more dilute samples indicate that bilayers in these samples are too large for their (apparent) size to be determined.

The abrupt micelle-to-bilayer transition demonstrates that the transition from micelles to bilayers is not a continuous change *via* a thermodynamically stable intermediate species. In accordance, SANS data in three samples near the micelle-to-bilayer transition, *i.e.* [$y = 0.30$, $c_t = 30$ mM], [$y = 0.35$, $c_t = 30$ mM] and [$y = 0.15$, $c_t = 15$ mM], could only be fitted assuming micelles, disks and vesicles to coexist (but not if either of these aggregate types were excluded). It is clearly seen that the fraction of micelles decreases as the solution mole fraction of DDAB (y) is increased at $c_t = 30$ mM, *i.e.* only micelles are present at $y = 0.25$, $f_m = 0.48$ at $y = 0.30$, $f_m = 0.33$ at $y = 0.35$ and only bilayers exist at $y = 0.40$. It is not possible to determine the micelle length of micelles coexisting with bilayers, since the scattering intensity in the low-q regime is completely dominated by the presence of the much larger bilayer aggregates. Examples of data for two samples where an appreciable amount of micelles are coexisting with bilayers can be seen in Fig. 2 [$y = 0.30$, $c_t = 30$ mM] and Fig. 3 [$y = 0.15$, $c_t = 15$ mM]. The coexistence of micelles and bilayer aggregates have previously been observed with SANS in similar surfactant systems.[23,25,32]

5. Rationalizing the growth of tablet-shaped micelles in terms of bending elasticity

In order to rationalize the formation and growth behaviour of generally shaped micelles, we have recently set up a theoretical model for the formation of triaxial tablet-shaped micelles, with distinct thickness, width and length (the general micelle model).[8] A schematic illustration of the geometrical shape of tablets we have considered is given in Fig. 5.

The free energy of a self-assembled interface as a function of mean and Gaussian curvature (H and K, respectively) may be obtained from the Helfrich-expression as[33]

$$\mathsf{E} = \gamma_0 A + 2k_c \int (H - H_0)^2 dA + \bar{k}_c \int K dA \qquad (18)$$

The first term on the right-hand side in eqn (18) ($= \gamma_0 A$) represents the free energy of stretching a self-assembled interface with area A and interfacial tension γ_0. The second and third terms take into account effects due to the dependence of free energy on the local curvature of the self-assembled interface, usually referred as to the bending free energy. According to the Gauss–Bonnet theorem, the last term in eqn (18) equals $4\pi\bar{k}_c$ for a geometrically closed interface and does not depend on the size of the self-assembled interfacial aggregate.

The Helfrich expression introduces three important parameters, or bending elasticity constants, related to different aspects of bending a surfactant self-assembled interface, *i.e.* the bending rigidity (k_c), the spontaneous curvature (H_0) and the saddle splay constant ($\bar{k}_c$). For thermodynamically stable objects, such as surfactant micelles and bilayers, the three bending elasticity constants may be interpreted as thermodynamic parameters, and they may be calculated from any suitable molecular model by means of minimizing the free energy per molecule of a surfactant interfacial layer at any given values of H and K.[6,7,9]

From eqn (18) it is possible to derive an expression of the free energy E of the tablet-shaped micelle shown in Fig. 5 as a function of the dimensionless length $l \equiv L/\xi$ and dimensionless half width $r \equiv R/\xi$, *i.e.*[8]

$$\frac{\mathsf{E}(r,l)}{kT} = \alpha + \delta\psi(r)\beta(\pi r + l) + 2r(\pi r + 2l)\lambda \qquad (19)$$

where $\lambda \equiv \xi^2\gamma_p/kT$ is the reduced and γ_p the real planar interfacial tension of the self-assembled interface. $\alpha \equiv 2\pi(3k_c + 2\bar{k}_c - 8\xi k_c H_0)/kT + 4\pi\lambda$, $\beta \equiv \pi k_c(1 - 4\xi H_0)/kT + 2\pi\lambda$ and $\delta \equiv 2\pi k_c/kT$ are three dimensionless parameters taking into account the bending free energy. The ψ-function ($0 < \psi < 1$) equals unity in the limit $r \to 0$ and zero as $r \to \infty$.[8,10]

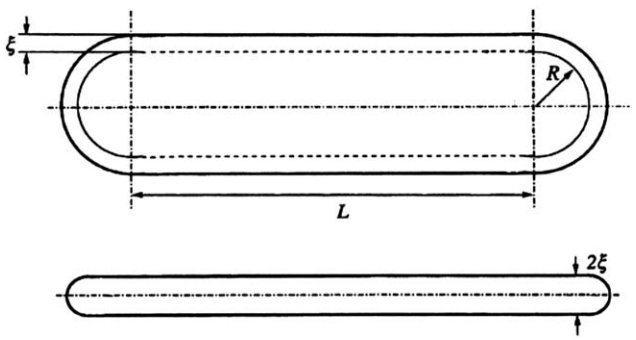

Fig. 5 Schematic illustration of a tablet-shaped micelle modelled as consisting of a central rectangular bilayer of thickness 2ξ, width $2R$ and length L with two half-circular ends with radius R. The bilayer part is surrounded by two straight half cylindrical rims of length L and radius ξ along its long sides and two semi-toroidal rim parts of radius ξ along the half circular ends of the micelle.

By means of taking into account the entropy of self-assembling surfactant molecules to form a dispersion of tablet-shaped micelles gives the following relation between the volume fraction of micelles ϕ_{mic} and bending elasticity constants,

$$\phi_{mic} = \frac{\pi\xi^6}{v^2}\int_0^\infty \frac{8r^2 + 6\pi r + \pi^2}{\beta + 4\lambda r} e^{-\delta\psi(r) - \pi\beta r - 2\pi\lambda r^2} dr \qquad (20)$$

From the length and width distribution function given in eqn (20) it is straightforward to calculate the average width $\langle\Omega\rangle \equiv 2(\langle R\rangle + \xi)$ and length $\langle\Lambda\rangle \equiv \langle L\rangle + \langle\Omega\rangle$, in a dispersed phase of tablet-shaped micelles, as functions of the different bending elasticity constants. Similarly, it is possible to estimate the bending elasticity constants from experimentally obtained values of micelle width and length.

It turns out that ξ and γ_p in eqn (20) are related to properties of a strictly planar self-assembled interface[6] and we may set the monolayer thickness equal to $\xi = a$ and the planar interfacial tension $\gamma_p = \gamma_0 + 2k_cH_0^2$ equal to a value that corresponds to the known volume fraction of micelles ϕ_{mic}. Remaining as unknown parameters in eqn (20) are the three bending elasticity constants H_0, k_c and $\bar{k}_c$. From our experimental data for general micelles we may only determine two independent parameters, namely the half axis related to width $b = \langle\Omega\rangle/2$ and half axis related to length $c = \langle\Lambda\rangle/2$, that are related to bending properties of the self-assembled interface. As a result, we cannot determine all three bending elasticity constants uniquely from our experimental data. However, we may make a rough estimate of k_cH_0, k_c and $\bar{k}_c$ from our experimentally obtained values of b and c by means of fixing the parameter $\beta \equiv \pi k_c(1 - 4\xi H_0)/kT + 2\pi\lambda$ to a certain value for a given surfactant concentration. It is known that β is mainly depending on the volume fraction of micelles and it must assume some positive value close to zero in order to yield reasonably large values of ϕ_{mic}.[8] Elongated micelles are expected to grow mainly in the length direction with increasing surfactant concentration and according to the general micelle model, $\beta = 0$ (or $\log\beta = -\infty$) at a given surfactant concentration, corresponds to the maximum size of the micelles and, as the surfactant concentration is increased, an abrupt transition to infinitely large cylinders is expected.[8]

In Fig. 6 we have plotted k_cH_0, k_c and $\bar{k}_c$, respectively, against the total mole fraction of DDAB (y) for some different values of β. We have chosen to plot k_cH_0, rather than H_0, since it is, from a molecular point of view, easier to interpret; k_cH_0 is directly related to the first moment in curvature and comparatively simple expressions may be derived from a suitable molecular model, whereas $H_0 \equiv k_cH_0/k_c$ is the ratio between the first and second moments with respect to H.[6,7,11] We obtain rather reasonable magnitudes of the values of all bending elasticity constants, *i.e.* k_c, $\bar{k}_c$ and ξk_cH_0 equal to a few kT. The bending rigidity k_c and the effective bending constant $k_{eff} \equiv 2k_c + \bar{k}_c$ are found to be always positive quantities as is required for self-assembled interfaces to be thermodynamically stable.[9,10] However, it seems as if the geometrical model shown in Fig. 5 somehow breaks down in the limit of small spheroidal micelles and we do not get reasonable values of the bending elasticity constants for the oblate DTAB micelles. Since β is expected to be approximately constant for a given total surfactant concentration, we may study the trends of the three bending elasticity constants as functions of the surfactant composition in order to rationalize the growth behaviour of general micelles in terms of the three bending elasticity constants.

The structural effect on composition in self-assembled interfacial aggregates formed by DTAB (one hydrocarbon chain per electric charge) and DDAB (two chains per electric charge) is expected to mainly depend on electrostatic properties, and so are trends in bending elasticity constants. The quantity k_cH_0, which is closely related to the spontaneous curvature, is found to decrease with an increasing fraction of DDAB. This particular trend turns out to mainly be the result of an increasing width of the micelles, and the concomitant reduction of curvature of the semitoriodal end caps of the tablets, with increasing values of y [*cf.* Fig. 4 and 6a]. The trend also agrees with recent molecular model calculations of k_cH_0 for mixtures of a single-chain and a double-chain ionic surfactant.[7] These calculations are based on the Poisson–Boltzmann mean field theory for charged self-assembled interfaces and take into account a finite thickness of the interface. In accordance, the reduction of k_cH_0 follows from the reduced charge density as a double-chain ionic surfactant, with larger area per aggregated surfactant, is admixed with a single-chain surfactant with identical charge number.

According to the general micelle model, the bending rigidity appears to mainly influence the length (or length-to-width ratio) of the micelles.[8] As a result, k_c is found to decrease in magnitude as the micelles grow in the length direction with an increasing fraction of DDAB [*cf.* Fig. 6b]. It is known that k_c is reduced by the sole effect of mixing two surfactants as a consequence of surfactant composition being a function of curvature.[7,34–36] Moreover, low k_c values (below about kT) are expected to favour geometrically heterogeneous aggregates, *i.e.* aggregates composed of geometrical parts that differ considerably in curvature, such as long wormlike or threadlike micelles and bilayer vesicles. As a result, surfactant micelles have frequently been observed to become substantially elongated in mixed surfactant systems.[37] As a matter of fact, threadlike micelles and unilamellar vesicles have frequently been observed in mixtures two oppositely charged surfactants, *i.e.* two surfactants with a pronounced asymmetry.[23,25,26,38] On the other hand, in our present system, with two cationic surfactants with similar head groups, the micelles are found to be rather small and compact, and bilayer disks are found to predominate over vesicles. These observations agree very well with recent model calculations showing that k_c is higher in the less asymmetric ionic/ionic (identical charge number) surfactant mixtures as compared to more asymmetric anionic/cationic surfactant mixtures.[7]

The saddle-splay constant has an indirect effect on the size of surfactant aggregates, in accordance with the Gauss-Bonnet theorem, and is seen to slightly decrease with an increasing fraction of DDAB in the micelles [*cf.* Fig. 6c]. This means that the growth rate of micelles is somewhat demoted by the influence of $\bar{k}_c$. From a molecular point of view the behaviour of the saddle-splay constant is rather complicated, but the electrostatic contribution to $\bar{k}_c$ has been found to slightly increase with an increasing fraction of double-chain surfactant in mixtures of a single-chain and double-chain ionic surfactant.[7]

In Fig. 6d we have also plotted the effective bending constant $k_{eff} \equiv 2k_c + \bar{k}_c$ as obtained from the growth behaviour of general tablet-shaped micelles. k_{eff} is a measure of the strength of the

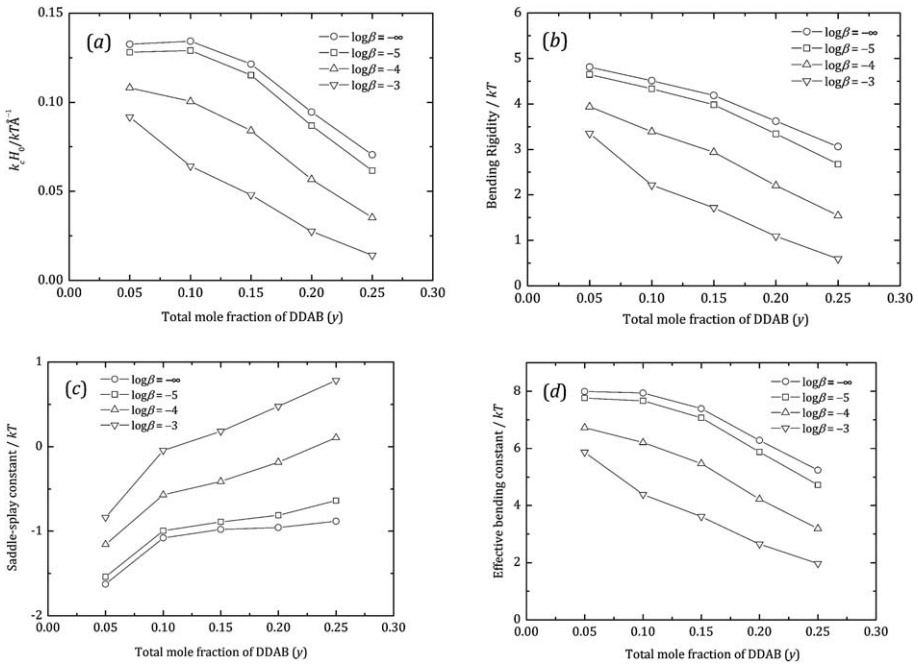

Fig. 6 Bending elasticity constants, as obtained from the fitting parameters b and c with a set equal to ξ, plotted against the total mole fraction of DDAB (y) for some given values of the thermodynamic parameter β. (a) Bending rigidity (k_c) times the spontaneous curvature (H_0), (b) bending rigidity (k_c), (c) saddle-splay constant ($\bar{k}_c$), (d) effective bending constant ($k_{eff} \equiv 2k_c + \bar{k}_c$). The symbols correspond to the samples $y = 0.05$, 0.10, 0.15, 0.20 and 0.25 at $c_t = 30$ mM.

driving force of self-assembling amphiphilic molecules and it must be a positive quantity for self-assembled interfacial aggregates to form at all. By means of taking into account effects due to the entropy of self-assembling surfactant molecules, it has been demonstrated that the aggregation number approaches unity as $k_{eff} \to 0$.[9,10] It is found that the behaviour of the k_{eff} *vs.* y plot in Fig. 6d is very similar to the behaviour of k_cH_0 in Fig. 6a. In general, the size of self-assembled interfacial aggregates increases with a decreasing spontaneous curvature (or decreasing k_cH_0) indicating that the behaviour of k_{eff} has a counteracting effect on the growth behaviour as generated by k_cH_0.

6. Conclusions

The growth behaviour of micelles, and their transformation to bilayer disks and vesicles, in mixtures of a single-chain (DTAB) and a double-chain cationic surfactant (DDAB) in heavy water (D_2O) have been investigated with SANS. Our observations are rationalized in terms of changes in surfactant mole fraction in the self-assembled interfacial aggregates. In accordance, the fraction of the surfactant with lowest cmc (DDAB) in the aggregates is found to considerably increase upon simply diluting a sample with given overall surfactant composition in the solution. It is found that DTAB form comparatively small oblate spheroidal micelles, which grow slightly in width and more significantly in length, with an increasing mole fraction of DDAB in the micelles, to form general triaxial micelles. The micelles do not grow larger than about 140 Å in the length direction. Instead they abruptly transform to form a dispersion of large bilayer aggregates. The micelle-to-bilayer transition appears to occur at a higher aggregate mole fraction of DDAB in D_2O ($x = 0.48$) as compared to H_2O ($x = 0.41$). Samples containing bilayers are found to predominantly consist of geometrically open bilayer disks or fragments coexisting with a smaller amount of geometrically closed unilamellar vesicles. The samples containing bilayers are found to consist of about 70–90% disks and 10–30% vesicles. In a few samples close to the micelle-to-bilayer transition micelles, disks and vesicles are observed to coexist.

The growth behaviour of the observed tablet-shaped micelles has been rationalized from the general micelle model, which combines theoretical approaches based on thermodynamics of self-assembly and bending elasticity, respectively. Our analyses suggest that small tablets grow slightly in the width direction, mainly as a result of a decreasing k_cH_0, as the mole fraction of DDAB is increased. On the other hand, the significant increase in length direction is found to be mainly the result of a decreasing bending rigidity (k_c), as an increasing fraction of DDAB is incorporated in the micelles. A more or less abrupt transition from micelles to bilayers at a spontaneous curvature $H_0 = 1/4\xi$, where ξ is the thickness of a self-assembled interface, is predicted by the general micelle model in excellent agreement with our experimental results.

Acknowledgements

This work was supported by the Swedish Research Council. The SANS measurements were supported by the European Commission (Grant agreement N 226507-NMI3).

References

1 M. Bergström and J. S. Pedersen, *Phys. Chem. Chem. Phys.*, 1999, **1**, 4437.
2 E. F. Marques, O. Regev, A. Khan, M. da Graça Miguel and B. Lindman, *J. Phys. Chem. B*, 1999, **103**, 8353.

3 M. Aratono, N. Onimaru, Y. Yoshikai, M. Shigehisa, I. Koga, K. Wongwailikhit, A. Ohta, T. Takiue, B. Lhoussaine, R. Strey, Y. Takata, M. Villeneuve and H. Matsubara, *J. Phys. Chem. B*, 2007, **111**, 107.
4 L. M. Bergström and M. Aratono, *Soft Matter*, 2011, **7**, 8870.
5 L. M. Bergström, *J. Colloid Interface Sci.*, 2006, **293**, 181.
6 L. M. Bergström, *Langmuir*, 2006, **22**, 3678.
7 L. M. Bergström, *Langmuir*, 2006, **22**, 6796.
8 L. M. Bergström, *ChemPhysChem*, 2007, **8**, 462.
9 L. M. Bergström, *Colloids Surf., A*, 2008, **316**, 15.
10 L. M. Bergström, *J. Colloid Interface Sci.*, 2008, **327**, 191.
11 L. M. Bergström, *Langmuir*, 2009, **25**, 1949.
12 J. P. Cotton, In *Neutron, X-Ray and Light Scattering: Introduction to an Investigative Tool For Colloidal and Polymeric Systems*, ed. P. Lindner and T. Zemb, North-Holland, Amsterdam, 1991, pp 19.
13 G. D. Wignall and F. S. Bates, *J. Appl. Crystallogr.*, 1986, **20**, 28.
14 J. S. Pedersen, *J. Phys. IV (Paris) Coll. C8*, 1993, **3**, 491.
15 J. S. Pedersen, D. Posselt and K. Mortensen, *J. Appl. Crystallogr.*, 1990, **23**, 321.
16 B. R. Bevington, *Data Reduction and Error Analysis for Physical Sciences*, McGraw-Hill, New York, 1969.
17 J. S. Pedersen, *Adv. Colloid Interface Sci.*, 1997, **70**, 171.
18 Y. Chevalier and T. Zemb, *Rep. Prog. Phys.*, 1990, **53**, 279.
19 M. Kotlarchyk and S. H. Chen, *J. Chem. Phys.*, 1983, **79**, 2461.
20 P. Mittelbach and G. Porod, *Acta Physica Austriaca*, 1962, **15**, 122.
21 J. B. Hayter and J. Penfold, *Mol. Phys.*, 1981, **42**, 409.
22 J. P. Hansen and J. B. Hayter, *Mol. Phys.*, 1982, **46**, 651.
23 M. Bergström and J. S. Pedersen, *J. Phys. Chem. B*, 2000, **104**, 4155.
24 O. Kratky and G. Porod, *J. Colloid Sci.*, 1949, **4**, 35.
25 M. Bergström, J. S. Pedersen, P. Schurtenberger and S. U. Egelhaaf, *J. Phys. Chem. B*, 1999, **103**, 9888.
26 M. Bergström and J. S. Pedersen, *J. Phys. Chem. B*, 1999, **103**, 8502.
27 T. Neugebauer, *Ann. Phys.*, 1943, **42**, 509.
28 M. Bergström and J. S. Pedersen, *Langmuir*, 1999, **15**, 2250.
29 C. Tanford, *J. Phys. Chem.*, 1972, **76**, 3020.
30 K. M. Lusvardi, A. P. Full and E. W. Kaler, *Langmuir*, 1995, **11**, 487.
31 S. S. Berr, *J. Phys. Chem.*, 1987, **91**, 4760.
32 J. S. Pedersen, S. U. Egelhaaf and P. Schurtenberger, *J. Phys. Chem.*, 1995, **99**, 1299.
33 W. Helfrich, *Z. Naturforsch. C*, 1973, **28**, 693.
34 M. M. Kozlov and W. Helfrich, *Langmuir*, 1992, **8**, 2792.
35 G. Porte and C. Ligoure, *J. Chem. Phys.*, 1995, **102**, 4290.
36 S. A. Safran, *Adv. Phys.*, 1999, **48**, 395.
37 M. Abe and J. F. Scamehorn, ed., *Mixed Surfactant Systems (Revised and Expanded)*, 2nd edn, CRC Press, 2004.
38 C. Tondre and C. Caillet, *Adv. Colloid Interface Sci.*, 2001, **93**, 115.